Multi-Modal Foundation Models for Computational Pathology: A Survey

Dong Li*
Baylor University
Waco, TX, USA
dong_li1@baylor.edu

Guihong Wan*
Harvard Medical School
Cambridge, MA, USA
guihong_wan@hsph.harvard.edu

Xintao Wu
University of Arkansas
Fayetteville, AR, USA
xintaowu@uark.edu

Xinyu Wu
Baylor University
Waco, TX, USA
xinyu_wu1@baylor.edu

Xiaohui Chen
Baylor University
Waco, TX, USA
xiaohui_chen1@baylor.edu

Yi He
William & Mary
Williamsburg, VA, USA
yihe@wm.edu

Christine G. Lian
Harvard Medical School
Cambridge, MA, USA
cglian@bwh.harvard.edu

Peter K. Sorger
Harvard Medical School
Cambridge, MA, USA
peter_sorger@hms.harvard.edu

Yevgeniy R. Semenov
Harvard Medical School
Cambridge, MA, USA
ysemenov@mgh.harvard.edu

Chen Zhao
Baylor University
Waco, TX, USA
chen_zhao@baylor.edu

Abstract

Foundation models have emerged as a powerful paradigm in computational pathology (CPath), enabling scalable and generalizable analysis of histopathological images. While early developments centered on uni-modal models trained solely on visual data, recent advances have highlighted the promise of multi-modal foundation models that integrate heterogeneous data sources such as textual reports, structured domain knowledge, and molecular profiles. In this survey, we provide a comprehensive and up-to-date review of multi-modal foundation models in CPath, with a particular focus on models built upon hematoxylin and eosin (H&E) stained whole slide images (WSIs) and tile-level representations. We categorize 32 state-of-the-art multi-modal foundation models into three major paradigms: vision-language, vision-knowledge graph, and vision-gene expression. We further divide vision-language models into non-LLM-based and LLM-based approaches. Additionally, we analyze 28 available multi-modal datasets tailored for pathology, grouped into image-text pairs, instruction datasets, and image-other modality pairs. Our survey also presents a taxonomy of downstream tasks, highlights training and evaluation strategies, and identifies key challenges and future directions. We aim for this survey to serve as a valuable resource for researchers and practitioners working at the intersection of pathology and AI.

Keywords

Computational Pathology, Foundation Model, Multi-Modality

1 Introduction

The advent of foundation models has significantly transformed computational pathology (CPath) by enabling scalable and generalizable deep learning solutions for analyzing histopathological images. These models are designed to extract meaningful patterns from vast collections of pathological data, enhancing diagnostic accuracy, prognostic assessments, and biomarker discovery [58]. Among various imaging modalities, hematoxylin and eosin

---

* Equal contribution.
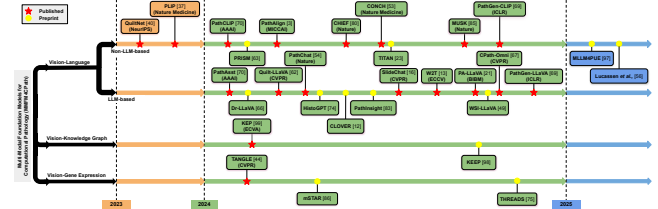
Figure 1: A roadmap of multi-modal foundation models for computational pathology (MMFM4CPath).

(H&E) stained images remain the most widely used in CPath due to their accessibility and effectiveness in capturing morphological details of tissues [11, 31]. Whole Slide Images (WSIs), obtained from high-resolution scanning of tissue samples, offer comprehensive histopathological insights but are computationally demanding due to their large size. To manage this, WSIs are typically divided into smaller tile images, which serve as the fundamental units for training deep learning models [16, 23, 80]. Existing foundation models for CPath (FM4CPath) can be broadly classified into uni-modal and multi-modal paradigms [47], with the former primarily focusing on visual representation learning and the latter integrating additional modalities such as text, knowledge graphs, and gene expression profiles for enhanced interpretability and performance.

Early research in CPath predominantly leveraged uni-modal foundation models [15, 76, 79], where deep learning models were trained solely on histopathological images. These uni-modal models have led to significant advancements in classification, segmentation, and prognostic prediction tasks by learning rich visual features from pathology slides. However, despite their success, these models are inherently limited by their exclusive reliance on image data, which often lacks crucial contextual information present in pathology reports, structured knowledge, or molecular profiles. To overcome these limitations, recent efforts have shifted toward multi-modal foundation models [53, 54, 80], which integrate heterogeneous data sources to provide more robust and interpretable insights.

Existing multi-modal foundation models for CPath (MMFM4CPath) can be categorized into three primary paradigms: vision-language,

Table 1: Comparison between our survey and related surveys. (V-L: Vision-Language, V-KG: Vision-Knowledge Graph, V-GE: Vision-Gene Expression, I-OM: Image-Other Modality)

Survey	# MMFM4CPath					# Datasets for MMFM4CPath				Tasks Taxo-nomy
	V-L		V-KG	V-GE	Total	Image-Text Pair	Instr-ution	I-OM	Total	
	Non-LLM	LLM								
Ochi *et, al.* [58]	4	0	0	1	5	4	0	1	5	✓
Chanda *et, al.* [11]	7	4	1	0	12	8	6	0	14	✗
Guan *et, al.* [31]	3	11	0	1	14	8	6	0	14	✗
Bilal *et, al.* [9]	8	4	0	2	14	0	0	0	0	✓
Li *et, al.* [47]	8	0	2	0	10	12	0	2	14	✓
This Survey	**13**	**14**	**2**	**3**	**32**	**12**	**12**	**4**	**28**	✓

vision-knowledge graph, and vision-gene expression models. A roadmap of up-to-date MMFM4CPath is shown in Figure 1. Vision-language models [37, 40, 67, 70] utilize textual annotations, such as WSI reports and tile-level captions, to enrich visual representations, facilitating zero-shot learning and seamless cross-modal integration between images and text. Within this category, models can be further divided into non-LLM-based and LLM-based approaches, with the latter incorporating large language models (LLMs) for improved natural language understanding and generative capabilities. Vision-knowledge graph models [98, 99] integrate structured domain knowledge by leveraging pathology-specific ontologies and knowledge graph to guide deep learning models. Vision-gene expression models [75, 86] align visual features with molecular-level insights from RNA sequencing and other omics data, facilitating genotype-phenotype associations for precision medicine.

While existing surveys have explored FM4CPath [9, 11, 31, 47, 58], they often lack a comprehensive analysis tailored to multi-modal approaches. As shown in Table 1, our survey differentiates itself by systematically categorizing 32 of the most up-to-date MMFM4CPath and analyzing 28 available multi-modal datasets for pathology, with an emphasis on modalities beyond vision-language integration. Additionally, we provide an in-depth discussion on evaluation methodologies, training strategies, and emerging challenges in this field. The key contributions of this survey include:

- **Comprehensive and Up-to-Date Survey.** This survey systematically reviews 32 multi-modal foundation models in computational pathology across vision-language, vision-knowledge graph, and vision-gene expression paradigms. It offers detailed comparisons of their architectures, pretraining strategies, and adaptation techniques, providing a broader and more current coverage than prior surveys.
- **In-Depth Analysis of Pathology-Specific Multi-Modal Datasets.** This survey curates and categorizes 28 available datasets into three types: image-text pairs, multi-modal instructions, and image-other modality pairs. We emphasize how these datasets enable various training strategies and highlight their roles in aligning modalities and supporting instruction tuning.
- **Thorough Overview of Multi-Modal Evaluation Tasks.** A taxonomy of evaluation tasks is provided, covering six major categories including classification, retrieval, generation, segmentation, prediction, and visual question answering. We detail how different MMFM4CPath are evaluated under various settings.
- **Future Research Opportunities.** We outline three promising directions, such as integrating H&E images with spatial omics data for deeper biological insight, leveraging H&E to predict MxIF markers for cost-effective virtual staining, and establishing

standardized benchmarks to ensure consistent evaluation across tasks and datasets. These directions aim to enhance the clinical relevance, scalability, and comparability of future models.

2 Background

2.1 Computational Pathology

Computational Pathology (CPath) is an interdisciplinary field that applies computational techniques, including machine learning and computer vision, to analyze and interpret pathological data. By leveraging digital pathology, CPath enhances diagnostic accuracy, facilitates large-scale biomarker discovery, and supports personalized medicine. Among the various imaging modalities in pathology, Hematoxylin and Eosin (H&E) stained images serve as the most commonly used vehicle for studying CPath. These images capture essential morphological characteristics of tissues, making them fundamental for histopathological analysis. Within the realm of digital pathology, Whole Slide Images (WSIs) and tile images are two primary forms of data representation. WSIs, generated from high-resolution scanning of entire tissue slides, provide comprehensive visual information at gigapixel scale, allowing pathologists to examine cellular structures in detail. However, due to their enormous size and high computational demands, WSIs pose significant challenges in terms of storage, processing, and analysis. To mitigate these challenges, WSIs are often divided into smaller, more manageable tile images, which serve as the primary unit of analysis in many computational pathology studies.

While visual analysis remains central to CPath, researchers increasingly rely on multi-modal data to enhance interpretability and improve model performance. One major auxiliary modality is language, which includes both tile-level captions that describe specific regions of tissue and WSI-level pathology reports that provide global contextual information about a slide. Integrating text data with images enables vision-language models to learn richer feature representations and facilitate interpretability. Another important modality is structured domain knowledge, often represented in knowledge graphs, which encode relationships between diseases, biomarkers, and tissue structures, guiding AI models toward more biologically plausible interpretations. Additionally, molecular data, such as gene expression profiles, offer complementary insights by linking histopathological features to underlying genetic mechanisms. By aligning visual data with gene expression information, vision-gene expression models enable the discovery of novel genotype-phenotype associations. Figure 2 illustrates examples of WSIs and tile images alongside the three major multi-modal paradigms in CPath. The synergy of these multi-modal approaches, including vision-language, vision-knowledge graph, and vision-gene expression, has proven crucial in advancing the field of CPath, enabling more robust, generalizable, and interpretable AI-driven pathology models.

2.2 Pre-training Objective for Multi-Modal FMs

Unlike uni-modal models, which are primarily pre-trained through self-supervised contrastive learning (SSCL). Multi-modal FMs, due
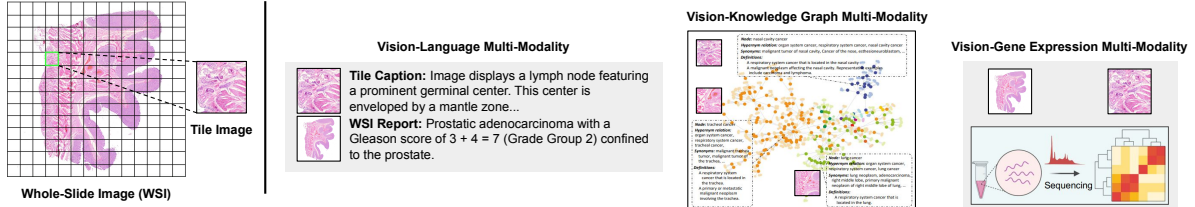
Figure 2: (Left) Illustration of whole-slide image and its corresponding tile images from H&E-stained tissue. (Right) The three primary types of multi-modal approaches in computational pathology.

to their cross-modal nature, involve a more diverse set of self-supervised learning (SSL) objectives during their pre-training process. Furthermore, when fine-tuning LLMs to enable conversational abilities, supervised instruction tuning is usually required.

The primary pre-training objective for multi-modal FMs is SSCL. CLIP [59], as a pioneer in this field, ensures that the embeddings generated by the image encoder and text encoder are as similar as possible for paired image-text data by utilizing contrastive loss. CoCa [89] builds upon CLIP by adding a multi-modal encoder and an additional captioning loss to enable the mapping from the visual space to the language space. BLIP-2 [48] trains a lightweight Querying Transformer (Q-Former) using a two-stage strategy. In the first stage, a frozen image encoder bootstraps vision-language representation learning, while in the second stage, visual features are mapped to the language model input space, leveraging a frozen LLM for text generation. Additionally, next word prediction (NWP) is a text-specific SSL task commonly used for fine-tuning LLMs. It aims to predict the most likely next token based on the given text sequence. Moreover, cross-modal alignment (CMA) multi-modal domain-specific task, which aims to build a unified semantic space where the embedding vectors from different modalities can reflect the same semantic content. In addition to contrastive learning, generative reconstruction and prediction are also commonly used SSL proxy tasks for CMA.

Instruction tuning (IT) is a method for fine-tuning LLMs to enable them to better understand and execute the instructions or task requirements provided by users. Unlike traditional pretraining objectives like NWP, the goal of IT is to enable the model to generate meaningful responses or actions based on specific instructions or questions. In Instruction Tuning, the model not only learns how to generate language but also learns how to adapt and generate different outputs according to various task requirements. This typically involves supervised training using a large number of instructions, ensuring that the model can understand the intent of the tasks and effectively perform them. Such tasks can include text generation, question answering, and conversation.

3 Multi-Modal Foundation Models for CPath

The power of multi-modal data has been repeatedly validated not only in the general machine learning community [78, 81, 82] but also in the field of computational pathology [11, 31, 58]. Given the high cost of pathology image data, leveraging other modalities—particularly textual data—as auxiliary information to learn more robust tile or WSI representations has become a dominant approach in developing foundation models for pathology (FM4CPath). Based on the modalities used, we categorize existing multi-modal

FM4CPath (MMFM4CPath) into three major groups: vision-language, vision-knowledge graph, and vision-gene expression models. Additionally, we comprehensively summarize their network architectures and pre-training details across different stages, as shown in Table 2. The rapid advancements in LLMs have enabled MMFM4CPath to possess enhanced generation and conversational capabilities. We further categorize vision-language models into non-LLM-based and LLM-based approaches. The goal of these methods is typically to learn robust representations of tiles or WSIs for a wide range of downstream tasks.

3.1 Non-LLM-Based Vision-Language FM4CPath

Vision-language FM4CPath enhance the models' understanding of pathological images by aligning paired image-text data under vision-language SSL frameworks, such as CLIP [59] and CoCa [89], enabling them to learn robust visual representations while also supporting zero-shot and cross-modal tasks. These methods typically use an out-of-shelf or trained vision encoder before performing joint visual-language pre-training, which has been shown to improve the performance [100]. They also leverage existing LLMs or Visual LLM (V-LLMs, *a.k.a.* MLLMs), typically in two ways: (i) fine-tuning them to serve as text encoders, or (ii) leaving them untuned, solely utilizing their capabilities for generation and conversation.

CLIP-based Vision-Language FM4CPath. The success of CLIP on natural images has inspired some works to apply it in the CPath domain. PLIP [37], PathCLIP [70] and QuiltNet [40] all fine-tune a CLIP model pre-trained on natural images using datasets composed of paired tiles and their captions. CHIEF [80] uses an image encoder pretrained for CPath domain [79] to encode the tile sequence extracted from WSIs to obtain WSI-level features and CLIP's text encoder to encode anatomical site information (WSI-level label). A weakly supervised aggregation network then combines both modalities to generate rich multi-modal WSI representations. Unlike previous methods that rely on out-of-shelf vision encoders, PathGen-CLIP [21] leverages the generative capabilities of V-LLMs to obtain high-quality tile-caption pairs and uses them to train an OpenAI CLIP [59] framework from scratch, followed by fine-tuning on tile-caption pairs from public datasets. PathAlign-R [3] is also trained from scratch on pathology data using the CLIP framework, but it focuses on the WSI-level. MLLM4PUE [97] leverages V-LLMs as the backbone to generate universal multi-modal embeddings for CPath, integrating images and text within a single framework to better understand their complex relationships.

CoCa-based Vision-Language FM4CPath. CoCa's multi-modal decoder serves as a crucial bridge between visual and linguistic information. By transforming encoded image features into text-aware

Table 2: Overview of architecture and pre-training details of MMFM4CPath

	Model (Availability)	Year	Vision (V)‡	Language (L) / Knowledge Graph (KG) / Gene Expression (GE)	Multi-Modal	Objective¶	V	O	M	Data Short Description	Input Image Type
Non-LLM-Based	QuiltNet [40] ✓	2023	T: ViT-B/32 ←[59]	L: Transformer Layers ←[59]	-	SSL (CLIP)	D	D	-	438K Tiles and 802K Captions	Tiles
	PLIP [37] ✓	2023	T: ViT-B/32 ←[59]	L: Transformer Layers ←[59]	-	SSL (CLIP)	D	D	-	208K Tile-Caption Pairs	Tiles
	PathCLIP [70] ✗	2024	T: ViT-B/32 ←[59]	L: Transformer Layers ←[59]	-	SSL (CLIP)	D	D	-	207K Tile-Caption Pairs	Tiles
	PRISM [63] ✗	2024	T: ViT-H/14 ←[76] W: Perceiver Net. [43]	L: BioGPT [57] (L1–12)	BioGPT [57] (L13–24) with Cross-Attention Layers	SSL (CoCa)	F,S	F	F,S	587K WSIs with 195K Specimens	WSIs
	PathAlign-R [3] ✗	2024	T: ViT-S/16 W: Q-Former [48]	L: Q-Former [48]	-	SSL (MSN) SSL (CLIP)	S,N F,S	N S	- -	Tiles From 354,089 WSIs 434k WSI-Report Pairs	WSIs
	PathAlign-G [3] ✗	2024	T: ViT-S/16 W: Q-Former [48]	L: Q-Former [48] L (LLM): PaLM-2 S [6]	MLP	SSL (MSN) SSL (BLIP-2) SSL (CMA)	S,N F,S F,D	N,N S,N N,F	N N S	Tiles From 354,089 WSIs 434k WSI-Report Pairs -	WSIs
	CHIEF [80] ✓	2024	T: Swin-T [52] ← [79] W: Aggregator Net.	L: Transformer Layers ←[59]	MLP	WSL (CLIP)	D,S	D	S	60K WSIs with Labels	WSIs
	CONCH [53] ✓	2024	T: ViT-B/16	L: Transformer Layers	Transformer Layers	SSL (iBOT) SSL (NWP) SSL (CoCa)	S N D	N S D	N S D	16M Tiles Sampled From 21K WSIs >950K Pathology Text Entries 1.17M Tile−Caption Pairs	Tiles
	TITAN [23] ✓	2024	T: ViT-L ←[53] W: ViT-S	L: Transformer Layers ←[53]	Transformer Layers ←[53]	SSL (iBOT) SSL (CoCa) SSL (CoCa)	F,S F,D F,D	N D D	N D D	336K WSIs 423K ROI-Caption Pairs 183K WSI-Report Pairs	WSIs
	MUSK [85] ✓	2025	T: V-FFN [65] Shared Attention Layers	L: L-FFN [65]	Cross-Attention Decoder	SSL (BEiT3) SSL (CoCa)	S D	S D	N S	1B Text Tokens and 50M Tiles 1.01M Tile−Caption Pairs	Tiles
	PathGen-CLIP [69] ✗	2025	T: ViT-B/32 ← [59]	L: Transformer Layers	-	SSL (CLIP) SSL (CLIP)	S D	S D	- -	1.6M High-Quality Tile-Caption Pairs 700K Tile-Caption Pairs	Tiles
	MLLM4PUE [97] ✗	2025	T: SigLIP [90] ←[50]	L: Qwen 1.5 [8]	MLP ←[50]	SSL (CLIP)	D	D	D	594K Tile-Caption Pairs	Tiles
	Lucassen et al. [56] ✗	2025	T: ViT-L/14 ←[15] W: Perceiver Net. [43]	L: BioGPT [57] (L1–12)	BioGPT [57] (L13–24) with Cross-Attention Layers	SSL (CoCa)	F,S	F	F,S	42K WSIs and 19K Reports	WSIs
Vision-Language / LLM-Based	PathAsst [70] ✗	2024	T: ViT-B/32 ←[70]	L (LLM): Vicuna-13B [17]	MLP	SSL (CMA) SL (IT)	F F	F I	S D	Description Part of PATHINSTRUCT 35K Samples From PATHINSTRUCT	Tiles
	Dr-LLaVA [66] ✓	2024	T: ViT-L/14 ←[59]	L (LLM): Vicuna-V1.5 [72]	MLP	SL (IT) & RL	D	I	D	Multi-turn Dialogues Based on 16K Tiles	Tiles
	Quilt-LLaVA [62] ✓	2024	T: ViT-B/32 ←[37]	L (LLM): GPT-4 [2]	MLP	SSL (CMA) SL (IT)	F F	F I	S D	723K Tile-Caption Pairs 107K Pathology-Specific Instructions	Tiles
	PathChat [54] ✓	2024	T: ViT-L/16 ←[15]	L (LLM): Llama 2-13B [73]	MLP with Attention Pooling	SSL (CoCa) SSL (CMA) SL (IT)	D F F	N F I	S D D	1.18M Tile-Caption Pairs ~100K Tile-Caption Pairs 457K Instructions with 999K VQA Turns	Tiles
	HistoGPT-S/M [74] ✓	2024	T: Swin-T [52] ←[79] W: Perceiver Net. [43]	L (LLM): BioGPT-B [57] / BioGPT-L [57]	-	WSL (MIL) SSL (NWP)	F,S F,F	F/F D/D	- -	15.1K WSIs with 6.7K Patient-Level Labels 15.1K WSI-Reports Pairs	Tiles
	HistoGPT-L [74] ✓	2024	T: ViT-L/16 ←[15] W: GCN [27]	L (LLM): BioGPT-L [57]	-	SSL (NWP)	F,S	S	-	15.1K WSI-Reports Pairs	Tiles
	CLOVER [12] ✓	2024	T: EVA-ViT-G/14 [25]	L: Q-Former [48] L (LLM): Vicuna 7B [17] / FlanT5XL [18]	Q-Former [48] MLP	SSL (BILP-2) SL (IT)	F F	S,N/N N,I/I	S,N N,S	438K Tiles and 802K Captions 45K VQA Instructions	Tiles
	PathInsight [83] ✓	2024	V-LLM: LLaVA [51] / Qwen-VL-7B [8] / InternLM [92]			SL (IT)		I / I / I		45K Instances Covering 6 Pathology Tasks	Tiles
	SlideChat [16] ✓	2024	T: ViT-L ←[53] W: LongNet [22]	L (LLM): Qwen2.5-7B [87]	MLP	SSL (CMA) SL (IT)	F,S F,D	F D	S D	4.2K WSI-Report Pairs 176K Instruction-Following VQA Pairs	WSIs
	W2T [13] ✓	2024	T: ViT-S ←[13, 24] / ResNet-50 ←[34] / HIPT [14] W: Transformer Layers	L: PubMedBERT [29] / BioClinicalBERT [30] / An Embedding Mapping	Transformer Layers	SSL (NWP)	T: F W: S	D D	S	804 WSIs with 7.14K VQA Pairs	WSIs
	PA-LLaVA [21] ✓	2024	T: ViT-B/32 ←[37]	L (LLM): LLama3 [28] with LoRA [36]	Transformer Layers	SSL (CLIP) SSL (CMA) SL (IT)	D F F	F I I	F D D	827K Tile-Caption Pairs 518K Tile-Caption Pairs 35.5K VQA Pairs	Tiles
	WSI-LLaVA [49] ✗	2024	T: ViT-G/14 W: LongNet [22] MLP	L: Bio_ClinicalBERT [5] L (LLM): Vicuna-7b-v1.5 [95]	MLP	SSL (CLIP) SSL (CMA) SL (IT)	F,F,S F,F,F F,F,F	D,N N,F N,I	N S D	9.85K WSI-Report Pairs 9.85K WSI-Report Pairs 175K VQA Pairs	WSIs
	CPath-Omni [67] ✗	2024	T: ViT-H/14 ←[100] ViT-L ←[59] W: SlideParser	L: Qwen2.5-14B [38]	MLP	SSL (CMA) SL (IT) SSL (CoCa) SL (IT)	F,F,F D,D,D F,F,D D,D,D	F I F I	S D F D	700K Tile-Caption Pairs 352K Tile Instructions 5.85K WSI-Report Pairs 53K Tile and 34K WSI Instructions	Tiles or WSIs
	PathGen-LLaVA [69] ✗	2025	T: ViT-B/32 ← [59]	L: Transformer Layers ← [59] L (LLM): Vicuna [17]	MLP	SSL (CLIP) SSL (CMA) SL (IC)	S F F	S,N N,F N,D	N S D	700K Tile-Caption Pairs 700K Tile-Caption Pairs 30K Detailed Tile Descriptions	Tiles
Vision-KG	KEP [99] ✓	2024	T: ViT-B/(16,32) ←[59, 93]	L: PubMedBERT [29] ←↰ KG: PubMedBERT [29]	-	SSL (PKE) SSL (CLIP)	N D	N,S D,F	- -	A Pathology KG with 50.5K Attributes 715K Tile-Caption Pairs	Tiles
	KEEP [98] ✓	2024	T: ViT-L/16 ←[15]	L, KG: PubMedBERT [29]	-	SSL (PKE) SSL (CLIP)	N D	S D	- -	A Pathology KG with 139K Attributes 143K Semantic Groups Through KG	Tiles
Vision-GE	TANGLE [44] ✓	2024	T: ViT-B (Rat) / Swin-T [52] (Human)←[79] W: ABMIL [41]	GE: A Three-Layer MLP	-	SSL (iBOT) SSL (CLIP)	S/N,N F/F,S	N D	- -	15M Rat Tiles From 47K WSIs 8.67K WSI- Gene Pairs	WSIs
	mSTAR [86] ✗	2024	T: ViT-L/16 ←[15] W: Two-Layer TransMIL [64]	L: BioBERT-Basev1.2 [46] GE: scBERT [88]	-	SSL (CLIP) SSL (SD)	F,S D,F	D,D N,N	- -	7.95K WSI-Report-Gene pairs 7.95K WSIs	WSIs
	THREADS [75] ✗	2025	T: ViT-L ←[53] W: ABMIL [41]	GE: scGPT [20] (RNA), A Four-Layer MLP (DNA)	-	SSL (CLIP)	F,S	D,S	-	26.6K WSI-Gene (RNA) Pairs & 20.5K WSI-Gene (DNA) Pairs	WSIs

† Network architecture types: T: Tile Encoder, W: WSI Encoder, L: Text Encoder, **LLM**: Large Language Model, **V-LLM**: Multi-modal LLM, **KG**: Knowledge Graph Encoder, **GE**: Gene Expression Encoder. Arrows (←) indicate the parameters initialization source of the architecture.

§ Multi-modal foundation models are typically pretrained in multiple stages, with **each row in this column representing a distinct pretraining phase**.

¶ Training objectives are categorized into Supervised Learning (**SL**), Weakly Supervised Learning (**WSL**), Self-Supervised Learning (**SSL**), and Reinforcement Learning (**RL**). SL includes Image Captioning (**IC**) and Instruction Tuning (**IT**), WSL includes Multiple Instance Learning (**MIL**), and SSL encompasses Contrastive Learning (**CL**), Masked Siamese Networks (**MSN**), Next Word Prediction (**NWP**), Cross-Modal Alignment (**CMA**), Pathology Knowledge Encoding (PKE), and Self-Distillation (**SD**). CL is further divided based on its contrastive objectives into **CLIP**, **CoCa**, **BLIP-2**, **iBOT** and **BEiT3**.

* Pre-training strategies for different architectures (**V**: Vision, **O**: Other Modalities, **M**: Multi-Modal): **F**: Frozen, **S**: From Scratch, **D**: Domain-Specific Tuning, **I**: Instruction Tuning, **N**: Not Used, -: Not Existed.

representations, it significantly boosts the cross-modal integration of MMFM4CPath, thereby enhancing its performance in advanced pathology applications. CONCH [53], PRISM [63], and Lucassen *et al.* [56] all pre-train an image encoder on pathology datasets, and then further conduct joint visio-language pre-training within the CoCa framework. The difference is that PRISM and Lucassen *et al.* extend the image encoder to the WSI-level using a Perceiver network [43] and employ WSIs along with their corresponding clinical reports for training. MUSK [85] first independently trains image and text encoders on unpaired pathology images and text tokens via masked data modeling within the BEiT-3 framework [77]. Using Masked Image Modeling (MIM) [33], it leverages ViT's patch structure to predict missing patches and learn robust representations, and then aligns the two modalities within the CoCa framework. TITAN [23] proposes a novel foundational framework for whole-slide imaging analysis through three progressive training stages: Initially, the WSI encoder is optimized via the iBOT framework [96] enhanced with positional encoding; this is followed by a dual-scaled refinement under the CoCa framework leveraging tile-level features and WSI-level contexts, where pathology-specialized V-LLMs generate diagnostic captions and structured reports.

Other Vision-Language FM4CPath. Unlike previous methods that use CLIP or CoCa framework, PathAlign-G [3] first pre-trains a ViT-S using Masked Siamese Networks (MSN) [7], and then fine-tunes the model using the BLIP-2 framework. This enables PathAlign-G to utilize a shared pathology image-text embedding space, enhancing its cross-modal capabilities and making it more suitable for generative tasks.

3.2 LLM-Based Vision-Language FM4CPath

The fusion of vision and language modalities provides an extra perspective for MMFM4CPath, where pathological visual representations aligned with language signals in latent space can assist LLMs in understanding pathology knowledge, thereby contributing to the construction of generative foundation AI assistants for pathologists [54]. These methods acquire pathology-specialized V-LLMs by pairing a pre-trained image encoder with an LLM via a simple multi-modal module for cross-modal feature alignment, then fine-tuning the LLM. Beyond contrastive learning, they employ diverse pre-training objectives, from supervised to self-supervised learning. We classify them into instruction-based and non-instruction-based methods based on LLM fine-tuning approaches.

Instruction-Based V-LLMs for CPath. Most V-LLMs for CPath undergo instruction tuning on carefully curated datasets, refining general-purpose LLMs for the pathology domain while enhancing their cross-modal understanding. PathAsst [70] builds a pathological V-LLM using PathCLIP as the visual backbone. It aligns the image encoder with the LLM via a trained layer on QA-based instructions, then fine-tunes the LLM with limited instructions. Following the same pre-training process, Quilt-LLaVA [62] and PA-LLaVA [21] are fine-tuned on their publicly available instruction-tuning datasets, while PathChat [54] undergoes instruction tuning on its carefully designed and diverse instructions. SlideChat [16] and WSI-LLaVA [49] go beyond the tile-level and create V-LLMs capable of handling gigapixel WSIs, and are fine-tuned on corresponding WSI-level instruction datasets.

Instead of relying on separate image encoders or vision-language architectures, PathInsight [83] directly fine-tunes existing V-LLMs using instructions covering six pathology tasks. In addition to instruction tuning, Dr-LLaVA [66] employs reinforcement learning (RL) with an automated reward function that assesses the clinical validity of responses during multi-turn interactions. CLOVER [12] aims to develop a cost-effective V-LLM for conversational pathology. It employs BLIP-2 with a lightweight Q-former [48], keeping both the visual encoder and LLM frozen to avoid full LLM tuning. CLOVER combines generation-based instructions from GPT-3.5 [2] with template-based instructions, forming hybrid instructions that improve understanding. As one of the most powerful models currently, CPath-Omni [67] aims to build a unified model that can process tile-level and WSI-level inputs separately through a proprietary framework, and integrate LLMs to enable generation and conversational capabilities. It undergoes four stages of training on three proposed datasets of different types: tile-caption pairs, tile-level instructions, and WSI-level instructions.

Non-Instruction-Based V-LLMs for CPath. PathGen-LLaVA [69] is trained from scratch on the CLIP architecture using tile-caption pairs, then a fully connected (FC) layer is trained to ensure the features extracted by the image encoder are understandable by the LLM. Finally, it employs a supervised image captioning task rather than instruction tuning, as PathGen-LLaVA is specifically designed for generating pathology image descriptions. W2T [13] utilizes four frozen visual extractors (including those trained on natural images and pathology images) and three text extractors in various combinations. It is trained on its proposed WSI-VQA instruction dataset using next word prediction (NWP) to interpret WSIs through generative visual question answering. HistoGPT [74] is designed with three model sizes: small, medium, and large. Among them, HistoGPT-S and HistoGPT-M first train a Perceiver Network [43] as a WSI encoder using multiple instance learning (MIL), followed by fine-tuning the LLM with NWP. HistoGPT-L, on the other hand, employs a graph convolutional network (GNN) [45] to encode WSI-level positional information, eliminating the need for a pre-trained WSI encoder. HistoGPT is capable of simultaneously generating reports from multiple pathology images and provides prompts that allow for expert knowledge guidance.

3.3 Enhancing FM4CPath with Other Modalities

Due to the high costs, pathology-specific datasets are typically small and sourced from diverse origins, such as websites or videos [37, 40]. This often results in noisy data with limited quality, making it unstructured and lacking domain knowledge. Meanwhile, massive multi-modal data aligned with clinical practices, along with domain-specific knowledge, such as gene expression profiles, remain underutilized for pretraining. Based on these, some studies have explored incorporating modalities beyond vision and language to enhance the training signal.

Vision-Knowledge Graph FM4CPath. To integrate structured domain-specific knowledge, KEP [99] constructs a pathology knowledge graph and encodes it using a knowledge encoder, which then guides vision-language pretraining. They design a pathology knowledge encoding (PKE) method to align semantic groups in the latent space for training the knowledge encoder. Similarly,

KEEP [98] builds a disease knowledge graph for encoding and employs knowledge-guided dataset structuring to generate tile-caption pairs for pretraining within the CLIP framework, incorporating strategies such as positive mining, hardest negative sampling, and false negative elimination.

Vision-Gene Expression FM4CPath. Serving as WSI-level information, gene expression profiles provide insights into quantitative molecular dynamics, complementing the qualitative morphological perspective of a WSI and capturing biologically and clinically significant details. TANGLE [44] is a transcriptomics-guided WSI representation learning framework that aligns image signals with RNA sequences encoded by multi-layer perceptron (MLP) in the latent space using contrastive loss, similar to CLIP. It extends beyond human tissues, incorporating a specialized architecture and dataset for rat tissue pretraining. THREADS [75], like TANGLE, utilizes molecular profiles from next-generation sequencing for WSI representation learning but uniquely integrates WSI-RNA and WSI-DNA sequence pairs. mSTAR [86] integrates three modalities within an extended CLIP framework, training on WSI-report-gene expression pairs via inter-modality and inter-cancer contrastive learning. It then employs self-distillation to transfer multi-modal knowledge to the patch extractor.

Note that some methods do not solely focus on pathology images but also encompass multi-modal medical imaging data such as Computed Tomography (CT), Magnetic Resonance Imaging (MRI), and X-ray from various organs [84, 91, 93, 94]. However, since their goal is not to leverage other medical image modalities to enhance pathology image representation but rather to develop a universal medical image model, these studies exceed the scope of our survey.

4 Multi-Modal Datasets for CPath

Larger, more diverse, and higher-quality datasets for CPath have been proven to be the key to the success of FM4CPath [76, 100], and MMFM4CPath is no exception. Curating pathology-specific public datasets has long been a challenge in this field, driving extensive research efforts. Many well-designed datasets have been developed to address various pathology-related questions, continuously advancing CPath. We summarize existing multi-modal datasets for CPath, highlighting high-quality datasets or those that have demonstrated success in current models. Based on data types, we categorize them into three groups as shown in Table 3.

Image-Text Pair Datasets for CPath. This category includes tile-level tile-caption pairs and WSI-level WSI-report pairs. Training on these datasets within a self-supervised contrastive learning framework enables FM4CPath to learn richer image embeddings while gaining zero-shot and cross-modal capabilities. Due to the expensive expert annotation and the preference of many research institutions for in-house data, several datasets have been constructed by collecting pathology tile images and text data from online sources, books, and publicly available educational resources. For example, QULIT [40], OPENPATH [37], ARCH [26] and MI-ZERO [55] leverage data from YouTube, Twitter, pathology textbooks, and educational resources, respectively. Due to the lack of a unified format, the collected data undergo standardized processing pipelines to ensure high quality. Image data is filtered for non-pathology images, followed by sub-figure segmentation. Text data is refined with LLMs,

including sub-caption segmentation and token-based filtering. Finally, multimodal models align figures with captions. Additionally, QULIT [40] uses speech recognition to extract text from videos.

Other tile-caption pair datasets primarily expand existing datasets or utilize internal datasets to enhance scale and diversity [21, 53, 67, 69, 70]. Notably, ARCH [26] is a multiple-instance captioning CPath dataset, where each image bag is associated with a single caption. Furthermore, datasets such as PATHGEN [69], HISTGEN [32], and MASS-340K [23] generate WSI-report pairs by leveraging generative models or processing WSI descriptions using LLMs.

Multi-Modal Instruction Datasets for CPath. These datasets incorporate diverse instructions for tuning LLM-based vision-language FM4CPath, training them as AI assistants in the pathology domain. Since manually designing instructions is typically expensive, instruction construction often directly relies on LLMs to generate cost-effective instruction datasets. The most common instruction type is VQA, which typically includes closed-ended and open-ended question-and-answer (Q&A) sessions to develop the model's conversational abilities. Due to prompt flexibility, different datasets create various instructions based on their needs. For example, PATHINSTRUCT[70] provides instruction-following samples that enable LLMs to call upon other pathology models for problem-solving. Lu *et al.*[54] developed six instruction types to adapt the model to diverse pathology conversation scenarios. CLOVER INSTRUCTION[12] generates instructions both through LLMs and by matching template questions with original text captions for cost-effectiveness. PATHMMU[68] uses enhanced descriptions with images to prompt GPT-4V [1], generating professional multi-modal pathology Q&As with detailed explanations. Due to the scarcity of large-scale multimodal pathology datasets for training WSI interpretation assistants, WSI-level instructions have emerged, typically creating VAQs from WSI reports and advanced LLM-generated prompts.

Image-Other Modality Pair Dataset. There is still a lack of extensive exploration of datasets involving vision and other modalities. Zhou *et al.* [98, 99] constructed two different disease knowledge graphs and, guided by one of them, created well-structured semantic groups linked through hierarchical relations. The MBTG-47K dataset [75] includes paired data of DNA and RNA gene sequences with WSIs. Xu et al. [86] publicly released a dataset with WSI-report-RNA-sequence pairs containing three modalities. These are bold attempts at constructing datasets that integrate pathology images with other modalities.

5 Evaluation Tasks

Unlike uni-modal FM4CPath, data from other modalities not only enhance MMFM4CPath's understanding of pathology images but also enable MMFM4CPath to perform zero-shot learning and cross-modal tasks. When MMFM4CPath are combined with LLMs, they gain the ability to engage in dialogue and generation, allowing them to adapt to more diverse tasks. We have summarized the evaluation tasks used by MMFM4CPath, as shown in Figure 3, and categorized them into six main types from a machine learning perspective: classification, retrieval, generation, segmentation, prediction, and visual question answering (VQA). Furthermore, we classify them based on the type of pathology image input they target (tile or WSI). For MMFM4CPath, their pre-training dataset and model design

Table 3: Multi-Modal Datasets for CPath.

Dataset[†] (Availability)	Data Type	Description	Staining[‡]	Dataset Invariant	Data Source Public	Private	Method	LLM Assisted
Quilt [40] ✓	Tile-Caption Pair	437,878 tiles paired with 802,144 captions extracted from 4,475 videos.	H, I, O	Quilt-1M: Combining Quilt with other pathology data sources to form 1M pairs.	YouTube	✗	QuiltNet [40]	✓
PathCap [70] ✓	Tile-Caption Pair	207K pathology tile-caption pairs.	H, I, O	-	PubMed [29]	✗	PathCLIP [70]	✓
OpenPath [70] ✓	Tile-Caption Pair	208,404 tile-caption pairs.	H, I, O	PathLAION: 32,041 additional tile–caption pairs scraped from the Internet and the LAION dataset [61]	WSI-Twitter, Replies, PathLAION	✗	PLIP [37]	✗
CONCH* [53] ✗	Tile-Caption Pair	1,170,647 tile–caption pairs.	H, I, O	-	PMC OA [42]	✓	CONCH [53]	✓
HistGen [32] ✓	WSI-Report Pair	A WSI-report dataset with 7,753 pairs.	H	-	TCGA [71]	✗	-	✓
Mass-340K [23] ✗	WSI	335,645 WSIs across 20 organs.	H, I	Synthetic captioning for 423,122 ROIs and curation of 182,862 WSI-report pairs.	GTEx [19]	✓	TITAN [23]	✓
CPath-Patch Caption [67] ✗	Tile-Caption Pair	700,145 tile-caption pairs from diverse datasets.	H, I, O	-	PathCap, Quilt-1M, OpenPath	✗	CPath-Omni [67]	✓
PathGen [69] ✓	Tile-Caption Pair	1.6 million high-quality tile-caption pairs from 7,300 WSIs.	H	PathGen$_{init}$: 700K tile-caption pairs from PathCap, OpenPath, and Quilt-1M	TCGA [71]	✗	PathGen-CLIP [69]	✓
Munich [74] ✗	WSI-Report Pair	15,129 paired WSIs and pathology reports from 6,705 patients.	H	-	-	✓	HistoGPT [74]	✗
PCaption-C [74] ✓	Tile-Caption Pair	1,409,058 tile-caption pairs.	H, I, O	PCaption-0.8M: removing non-human pathology data and PCaption-0.5M: further filter out pairs with <20 words.	PMC-OA [42], Quilt-1M	✗	PA-LLaVA [21]	✓
ARCH [26] ✓	Bag-Caption Pair	11,816 bags and 15,164 images, with each bag containing multiple tiles.	H, I	-	PubMed [29], pathology textbooks	✗	-	✗
MI-Zero [55] ✓	Tile-Caption Pair	Diverse dataset of 33,480 tile-caption pairs.	H, I, O	-	educational resources, ARCH	✗	-	✗
PathInstruct [70] ✓	Tile-Level Instruction	180K pathology multi-modal instruction-following samples.	H, I, O	-	YouTube	✗	PathAsst [54]	✓
CPath-Patch Instruction [67] ✗	Tile-Level Instruction	351,871 tile-level samples, including tile-caption pairs, VQA pairs, labeled images for classification, and visual referring prompting pairs.	H	CPath-VQA: created by generating VQA pairs using GPT-4o [39], which combines classification labels with image data for datasets lacking captions.	CPath-VQA, PathGen, CPath-PatchCaption, PathInstruct	✓	CPath-Omni [67]	✓
CPath-WSI Instruction [67] ✗	WSI-Level Instruction	7,312 WSI-level samples, including captioning, VQA, and classification.	H	Further generate a WSI VQA dataset by prompting GPT-4 [2].	HistGen	✗	CPath-Omni [67]	✓
Qulit-Instruct [62] ✓	VQA Pair	107,131 question/answer pairs.	H, I, O	QUILT-VQA: a Q&A dataset from Youtube videos, categorized into image-dependent and general-knowledge questions; QUILT-VQA-red: QUILT-VQA with red circle marking the ROI in the pathology image.	YouTube	✗	Quilt-LLaVA [62]	✓
PathChat* [54] ✗	Tile-Level Instruction	456,916 instructions with 999,202 question and answer turns.	H, I	PathQABench: an expert-curated benchmark of 105 high-resolution pathology images, split into PathQABench-Public and PathQABench-Private subsets.	PMC-OA [42], TCGA [71]	✓	PathChat [54]	✓
CLOVER Instruction [12] ✓	Tile-Level Instruction	45K question-and-answer instructions.	H	-	Quilt-VQA, PathVQA [35]	✓	CLOVER [12]	✓
Path-EnhanceDS [83] ✓	Tile-Level Instruction	49K tile-level instructions, including captioning, VQA, classification and conversation.	H	-	OpenPath, TCGA [71], PathVQA [35], etc.	✗	PathInsight [83]	✓
Slide-Instruction [16] ✓	WSI-Level Instruction	44,181 WSI-caption pairs and 175,754 visual Q&A pairs.	H	SlideBench: 734 WSI captions along with a substantial number of closed-set VQA pairs to establish evaluation benchmark.	TCGA [71]	✗	SlideChat [16]	✓
WSI-VQA [13] ✓	VQA Pair	977 WSIs and 8,672 Q&A pairs.	H	-	TCGA-BRCA [71]	✗	W2T [13]	✓
PA-LLaVA* [21] ✓	VQA Pair	35,543 question-answer pairs.	H	-	PathVQA [35]	✗	PA-LLaVA [21]	✓
WSI-Bench [49] ✗	VQA Pair	179,569 WSI-level VQA pairs, which span across 3 pathological capabilities with 11 tasks.	H	SlideBench: 734 WSI captions along with a substantial number of closed-set VQA pairs to establish evaluation benchmark.	TCGA [71]	✗	WSI-LLaVA [49]	✓
PathMMU [68] ✓	VQA Pair	33,428 Q&As along with 24,067 pathology images.	H, I, O	SlideBench: 734 WSI captions along with a substantial number of closed-set VQA pairs to establish evaluation benchmark.	PubMed [29], Quilt-1M, Atlas [4], OpenPath	✗	-	✓
KEEP* [98] ✓	Pathology KG	KG contains 11,454 disease entities and 139,143 associated attributes.	-	-	DO [60], UMLS [10]	✗	KEEP [98]	✓
	Pathology Semantic Group	143K pathology semantic groups linked through the disease KG	H, I, O	-	Quilt-1M, OpenPath	✗		
PathKT [99] ✓	Pathology KG	Pathology KG that consists of 50,470 informative attributes	-	-	OncoTree	✗	KEP [99]	✗
mSTAR* [86] ✓	WSI-Report-RNA-Seq Pair	A dataset with 7,947 cases with image, text and RNA sequence modalities for pretraining.	H	-	TGCA [71]	✗	mSTAR [86]	✓
MBTG-47K [75] ✗	WSI-RNA-Seq Pair WSI-DNA-Seq Pair	26,615 WSI-RNA pairs, and 20,556 WSI-DNA pairs.	H	-	TCGA [71], GTEx [19]	✓	THREADS [75]	✗

The row groups on the left are labeled: **Image-Text Pair**, **Multi-Modal Instruction**, **Image-Other Modality**.

[†] Some methods introduced datasets without naming them, so we use the method name instead and marked with an asterisk (*).
[‡] Staining type: **H**: H&E, **I**: IHC, **O**: Others.

are closely tied to their evaluation tasks. For example, benefiting from multi-scale and more diverse training instructions, CPath-Omni [67] has been evaluated across the widest range of tasks.

Classification is the most common evaluation task for MMFM4CPath, as many pathology-related tasks, such as cancer subtyping and biomarker prediction, are fundamentally classification problems. Most MMFM4CPath are evaluated on classification tasks across

various settings. Models using tile-level inputs can perform WSI-level classification via multiple instance learning (MIL), treated as weakly supervised due to the lack of detailed region annotations. Multi-modal data enables zero-shot or few-shot classification with minimal reliance on costly annotations. Some methods also assess out-of-distribution (OOD) generalization to handle distribution shifts between training and test data (e.g., data collected
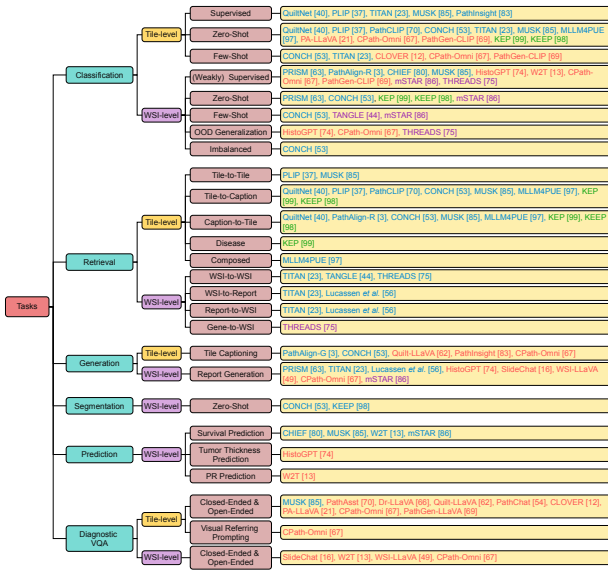
Figure 3: A comprehensive taxonomy of MMFM4CPath, categorized according to evaluation tasks. Non-LLM-based vision-language, LLM-based vision-language, vision-knowledge graph, and vision-gene expression models are highlighted in different colors, respectively.

from different institutions). Additionally, CONCH [53] evaluates classification on rare diseases with imbalanced data.

In addition to basic image-to-image retrieval, non-LLM-based MMFM4CPath are widely used for cross-modal retrieval tasks, such as text-to-image and image-to-text retrieval. KEP [99] performs one-to-many disease retrieval, retrieving captions or tiles with the same disease label using disease names. MLLM4PUE [97] enables many-to-one composed retrieval by using pathology images and questions as queries. Moreover, due to its capability to understand gene expression data, THREADS [75] generates class prompts from gene expression profiles for WSI retrieval.

The integration of LLMs, whether by fine-tuning them as part of the model's architecture or by directly utilizing existing models, enables MMFM4CPath to generate captions/reports from tiles/WSIs. CONCH [53] and KEP [99] evaluate the segmentation capabilities of these models. Some MMFM4CPath have also been tested for prediction tasks, using WSIs to generate continuous value predictions.

LLM-based MMFM4CPath models focus on evaluating their diagnostic VQA ability. Compared to traditional QA tasks, VQA incorporates pathology images into its questions, challenging the image understanding capabilities of V-LLMs. Typically, VQA tasks involve answers from a fixed set, usually in the form of closed-ended questions, such as multiple-choice (single or multiple answers) or true/false questions, as well as open-ended questions with no predefined answer options. These tasks can also be divided into multi- and single-turn dialogues. The initial LLM-based MMFM4CPath only performed tile-level VQA tasks [54, 70], but recently, conversational abilities on WSI have gained increasing attention [16, 49]. Additionally, CPath-Omni [67] has been validated on the visual referring prompting task, where the regions of interest (ROIs) are highlighted, and both the question and answer are based on the

these regions. It is worth noting that, due to its flexible format, the VQA task offers high adaptability: tasks like classification and generation can be transformed into VQA tasks via prompt engineering [67, 83]. Thus, LLM-based MMFM4CPath also encompass evaluation capabilities typical of non-LLM-based models. In addition to the quantitative analysis above, qualitative analysis is also frequently used to assess the performance of MMFM4CPath, especially their VQA and generation abilities. This is done by directly observing or through evaluation by professional pathologists to assess the quality of the generated text.

6 Future Directions

Developing MMFM4CPath Integrating H&E Images with Spatial Omics. The integration of H&E-stained histopathology images with spatial omics data, such as spatial transcriptomics and proteomics, represents a promising frontier in computational pathology. By coupling morphological context with spatially resolved molecular signatures, future multi-modal foundation models could enable precise cellular localization of gene and protein expression, bridging the gap between tissue architecture and molecular mechanisms. Developing such models would require addressing challenges like data sparsity, spatial resolution mismatch, and alignment between modalities, but could significantly enhance our understanding of disease heterogeneity and microenvironmental interactions.

Developing MMFM4CPath to Predict MxIF Markers from H&E Images. A compelling direction involves using H&E images to predict marker expressions captured by multiplexed immunofluorescence (MxIF), enabling cost-effective and scalable estimation of protein-level biomarkers. This line of research leverages the morphological cues from H&E to infer high-dimensional proteomic data, potentially reducing the need for expensive MxIF experiments. Multi-modal foundation models trained with paired H&E-MxIF data could facilitate virtual staining or marker imputation, supporting downstream tasks such as subtyping, immune landscape assessment, and therapy response prediction in a non-invasive manner.

Standardized Benchmarking for MMFM4CPath. As the field matures, there is a pressing need to establish standardized metrics and unified benchmarks for evaluating MMFM4CPath. Current evaluations are fragmented across tasks, modalities, and datasets, limiting comparability and reproducibility. Future work should focus on developing comprehensive evaluation protocols that span classification, retrieval, generation, and VQA across tile- and WSI-level inputs. Such efforts would guide model development, ensure fair comparisons, and accelerate the translation of multi-modal models into clinical practice.

7 Conclusion

In this survey, we have systematically reviewed the recent advances in multi-modal foundation models for computational pathology, focusing on three major paradigms: vision-language, vision-knowledge graph, and vision-gene expression models. We categorized 32 state-of-the-art models, analyzed 28 multi-modal datasets, and summarized key downstream tasks and evaluation strategies. Our comprehensive comparison highlights the growing impact and promise of integrating diverse data modalities in computational pathology.

References

[1] 2023. GPT-4V(ision) System Card. https://api.semanticscholar.org/CorpusID: 263218031

[2] Josh Achiam, Steven Adler, Sandhini Agarwal, Lama Ahmad, Ilge Akkaya, Florencia Leoni Aleman, Diogo Almeida, Janko Altenschmidt, Sam Altman, Shyamal Anadkat, et al. 2023. Gpt-4 technical report. *arXiv preprint arXiv:2303.08774* (2023).

[3] Faruk Ahmed, Andrew Sellergren, Lin Yang, Shawn Xu, Boris Babenko, Abbi Ward, Niels Olson, Arash Mohtashamian, Yossi Matias, Greg S Corrado, et al. 2024. Pathalign: A vision-language model for whole slide images in histopathology. *arXiv preprint arXiv:2406.19578* (2024).

[4] Maximilian Alber, Stephan Tietz, Jonas Dippel, Timo Milbich, Timothée Lesort, Panos Korfiatis, Moritz Krügener, Beatriz Perez Cancer, Neelay Shah, Alexander Möllers, et al. 2025. A Novel Pathology Foundation Model by Mayo Clinic, Charit\'e, and Aignostics. *arXiv preprint arXiv:2501.05409* (2025).

[5] Emily Alsentzer, John R Murphy, Willie Boag, Wei-Hung Weng, Di Jin, Tristan Naumann, and Matthew McDermott. 2019. Publicly available clinical BERT embeddings. *arXiv preprint arXiv:1904.03323* (2019).

[6] Rohan Anil, Andrew M Dai, Orhan Firat, Melvin Johnson, Dmitry Lepikhin, Alexandre Passos, Siamak Shakeri, Emanuel Taropa, Paige Bailey, Zhifeng Chen, et al. 2023. Palm 2 technical report. *arXiv preprint arXiv:2305.10403* (2023).

[7] Mahmoud Assran, Mathilde Caron, Ishan Misra, Piotr Bojanowski, Florian Bordes, Pascal Vincent, Armand Joulin, Mike Rabbat, and Nicolas Ballas. 2022. Masked siamese networks for label-efficient learning. In *European conference on computer vision*. Springer, 456–473.

[8] Jinze Bai, Shuai Bai, Shusheng Yang, Shijie Wang, Sinan Tan, Peng Wang, Junyang Lin, Chang Zhou, and Jingren Zhou. 2023. Qwen-vl: A frontier large vision-language model with versatile abilities. *arXiv preprint arXiv:2308.12966* 1, 2 (2023), 3.

[9] Mohsin Bilal, Manahil Raza, Youssef Altherwy, Anas Alsuhaibani, Abdulrahman Abduljabbar, Fahdah Almarshad, Paul Golding, Nasir Rajpoot, et al. 2025. Foundation Models in Computational Pathology: A Review of Challenges, Opportunities, and Impact. *arXiv preprint arXiv:2502.08333* (2025).

[10] Olivier Bodenreider. 2004. The unified medical language system (UMLS): integrating biomedical terminology. *Nucleic acids research* 32, suppl_1 (2004), D267–D270.

[11] Dibaloke Chanda, Milan Aryal, Nasim Yahya Soltani, and Masoud Ganji. 2024. A New Era in Computational Pathology: A Survey on Foundation and Vision-Language Models. *arXiv preprint arXiv:2408.14496* (2024).

[12] Kaitao Chen, Mianxin Liu, Fang Yan, Lei Ma, Xiaoming Shi, Lilong Wang, Xiaosong Wang, Lifeng Zhu, Zhe Wang, Mu Zhou, et al. 2024. Cost-effective instruction learning for pathology vision and language analysis. *arXiv preprint arXiv:2407.17734* (2024).

[13] Pingyi Chen, Chenglu Zhu, Sunyi Zheng, Honglin Li, and Lin Yang. 2024. Wsi-vqa: Interpreting whole slide images by generative visual question answering. In *European Conference on Computer Vision*. Springer, 401–417.

[14] Richard J Chen, Chengkuan Chen, Yicong Li, Tiffany Y Chen, Andrew D Trister, Rahul G Krishnan, and Faisal Mahmood. 2022. Scaling vision transformers to gigapixel images via hierarchical self-supervised learning. In *Proceedings of the IEEE/CVF conference on computer vision and pattern recognition*. 16144–16155.

[15] Richard J Chen, Tong Ding, Ming Y Lu, Drew FK Williamson, Guillaume Jaume, Andrew H Song, Bowen Chen, Andrew Zhang, Daniel Shao, Muhammad Shaban, et al. 2024. Towards a general-purpose foundation model for computational pathology. *Nature Medicine* (2024).

[16] Ying Chen, Guoan Wang, Yuanfeng Ji, Yanjun Li, Jin Ye, Tianbin Li, Bin Zhang, Nana Pei, Rongshan Yu, Yu Qiao, et al. 2024. SlideChat: A Large Vision-Language Assistant for Whole-Slide Pathology Image Understanding. *arXiv preprint arXiv:2410.11761* (2024).

[17] Wei-Lin Chiang, Zhuohan Li, Ziqing Lin, Ying Sheng, Zhanghao Wu, Hao Zhang, Lianmin Zheng, Siyuan Zhuang, Yonghao Zhuang, Joseph E Gonzalez, et al. 2023. Vicuna: An open-source chatbot impressing gpt-4 with 90%* chatgpt quality. *See https://vicuna. lmsys. org (accessed 14 April 2023)* 2, 3 (2023), 6.

[18] Hyung Won Chung, Le Hou, Shayne Longpre, Barret Zoph, Yi Tay, William Fedus, Yunxuan Li, Xuezhi Wang, Mostafa Dehghani, Siddhartha Brahma, et al. 2024. Scaling instruction-finetuned language models. *Journal of Machine Learning Research* 25, 70 (2024), 1–53.

[19] GTEx Consortium, Kristin G Ardlie, David S Deluca, Ayellet V Segrè, Timothy J Sullivan, Taylor R Young, Ellen T Gelfand, Casandra A Trowbridge, Julian B Maller, Taru Tukiainen, et al. 2015. The Genotype-Tissue Expression (GTEx) pilot analysis: multitissue gene regulation in humans. *Science* 348, 6235 (2015), 648–660.

[20] Haotian Cui, Chloe Wang, Hassaan Maan, Kuan Pang, Fengning Luo, Nan Duan, and Bo Wang. 2024. scGPT: toward building a foundation model for single-cell multi-omics using generative AI. *Nature Methods* 21, 8 (2024), 1470–1480.

[21] Dawei Dai, Yuanhui Zhang, Long Xu, Qianlan Yang, Xiaojing Shen, Shuyin Xia, and Guoyin Wang. 2024. Pa-llava: A large language-vision assistant for human pathology image understanding. In *2024 IEEE International Conference on Bioinformatics and Biomedicine (BIBM)*. IEEE, 3138–3143.

[22] Jiayu Ding, Shuming Ma, Li Dong, Xingxing Zhang, Shaohan Huang, Wenhui Wang, Nanning Zheng, and Furu Wei. 2023. Longnet: Scaling transformers to 1,000,000,000 tokens. *arXiv preprint arXiv:2307.02486* (2023).

[23] Tong Ding, Sophia J Wagner, Andrew H Song, Richard J Chen, Ming Y Lu, Andrew Zhang, Anurag J Vaidya, Guillaume Jaume, Muhammad Shaban, Ahrong Kim, et al. 2024. Multimodal whole slide foundation model for pathology. *arXiv:2411.19666* (2024).

[24] Alexey Dosovitskiy. 2020. An image is worth 16x16 words: Transformers for image recognition at scale. *arXiv preprint arXiv:2010.11929* (2020).

[25] Yuxin Fang, Wen Wang, Binhui Xie, Quan Sun, Ledell Wu, Xinggang Wang, Tiejun Huang, Xinlong Wang, and Yue Cao. 2023. Eva: Exploring the limits of masked visual representation learning at scale. In *Proceedings of the IEEE/CVF conference on computer vision and pattern recognition*. 19358–19369.

[26] Jevgenij Gamper and Nasir Rajpoot. 2021. Multiple instance captioning: Learning representations from histopathology textbooks and articles. In *Proceedings of the IEEE/CVF conference on computer vision and pattern recognition*. 16549–16559.

[27] Rushin H Gindra, Yi Zheng, Emily J Green, Mary E Reid, Sarah A Mazzilli, Daniel T Merrick, Eric J Burks, Vijaya B Kolachalama, and Jennifer E Beane. 2024. Graph perceiver network for lung tumor and bronchial premalignant lesion stratification from histopathology. *The American Journal of Pathology* 194, 7 (2024), 1285–1293.

[28] Aaron Grattafiori, Abhimanyu Dubey, Abhinav Jauhri, Abhinav Pandey, Abhishek Kadian, Ahmad Al-Dahle, Aiesha Letman, Akhil Mathur, Alan Schelten, Alex Vaughan, et al. 2024. The llama 3 herd of models. *arXiv preprint arXiv:2407.21783* (2024).

[29] Yu Gu, Robert Tinn, Hao Cheng, Michael Lucas, Naoto Usuyama, Xiaodong Liu, Tristan Naumann, Jianfeng Gao, and Hoifung Poon. 2021. Domain-specific language model pretraining for biomedical natural language processing. *ACM Transactions on Computing for Healthcare (HEALTH)* 3, 1 (2021), 1–23.

[30] Yu Gu, Robert Tinn, Hao Cheng, Michael Lucas, Naoto Usuyama, Xiaodong Liu, Tristan Naumann, Jianfeng Gao, and Hoifung Poon. 2021. Domain-specific language model pretraining for biomedical natural language processing. *ACM Transactions on Computing for Healthcare (HEALTH)* 3, 1 (2021), 1–23.

[31] Xianchao Guan, Zheng Zhang, Yifeng Wang, and Yongbing Zhang. 2025. A systematic review on Multimodal Large Language Models (MLLMs) in computational pathology. *Authorea Preprints* (2025).

[32] Zhengrui Guo, Jiabo Ma, Yingxue Xu, Yihui Wang, Liansheng Wang, and Hao Chen. 2024. Histgen: Histopathology report generation via local-global feature encoding and cross-modal context interaction. In *International Conference on Medical Image Computing and Computer-Assisted Intervention*. Springer, 189–199.

[33] Kaiming He, Xinlei Chen, Saining Xie, Yanghao Li, Piotr Dollár, and Ross Girshick. 2022. Masked autoencoders are scalable vision learners. In *CVPR*.

[34] Kaiming He, Xiangyu Zhang, Shaoqing Ren, and Jian Sun. 2016. Deep residual learning for image recognition. In *Proceedings of the IEEE conference on computer vision and pattern recognition*. 770–778.

[35] Xuehai He, Yichen Zhang, Luntian Mou, Eric Xing, and Pengtao Xie. 2020. Pathvqa: 30000+ questions for medical visual question answering. *arXiv preprint arXiv:2003.10286* (2020).

[36] Edward J Hu, Yelong Shen, Phillip Wallis, Zeyuan Allen-Zhu, Yuanzhi Li, Shean Wang, Lu Wang, Weizhu Chen, et al. 2022. Lora: Low-rank adaptation of large language models. *ICLR* 1, 2 (2022), 3.

[37] Zhi Huang, Federico Bianchi, Mert Yuksekgonul, Thomas J Montine, and James Zou. 2023. A visual–language foundation model for pathology image analysis using medical twitter. *Nature medicine* (2023).

[38] Binyuan Hui, Jian Yang, Zeyu Cui, Jiaxi Yang, Dayiheng Liu, Lei Zhang, Tianyu Liu, Jiajun Zhang, Bowen Yu, Keming Lu, et al. 2024. Qwen2. 5-coder technical report. *arXiv preprint arXiv:2409.12186* (2024).

[39] Aaron Hurst, Adam Lerer, Adam P Goucher, Adam Perelman, Aditya Ramesh, Aidan Clark, AJ Ostrow, Akila Welihinda, Alan Hayes, Alec Radford, et al. 2024. Gpt-4o system card. *arXiv preprint arXiv:2410.21276* (2024).

[40] Wisdom Ikezogwo, Saygin Seyfioglu, Fatemeh Ghezloo, Dylan Geva, Fatwir Sheikh Mohammed, Pavan Kumar Anand, Ranjay Krishna, and Linda Shapiro. 2024. Quilt-1m: One million image-text pairs for histopathology. *NeurIPS* (2024).

[41] Maximilian Ilse, Jakub Tomczak, and Max Welling. 2018. Attention-based deep multiple instance learning. In *International conference on machine learning*. PMLR, 2127–2136.

[42] Ana-Maria Istrate, Donghui Li, Dario Taraborelli, Michaela Torkar, Boris Veytsman, and Ivana Williams. 2022. A large dataset of software mentions in the biomedical literature. *arXiv preprint arXiv:2209.00693* (2022).

[43] Andrew Jaegle, Felix Gimeno, Andy Brock, Oriol Vinyals, Andrew Zisserman, and Joao Carreira. 2021. Perceiver: General perception with iterative attention. In *ICML*. PMLR.

[44] Guillaume Jaume, Lukas Oldenburg, Anurag Vaidya, Richard J Chen, Drew FK Williamson, Thomas Peeters, Andrew H Song, and Faisal Mahmood. 2024. Transcriptomics-guided slide representation learning in computational pathology. In *CVPR*.

[45] Thomas N Kipf and Max Welling. 2016. Semi-supervised classification with graph convolutional networks. *arXiv preprint arXiv:1609.02907* (2016).

[46] Jinhyuk Lee, Wonjin Yoon, Sungdong Kim, Donghyeon Kim, Sunkyu Kim, Chan Ho So, and Jaewoo Kang. 2020. BioBERT: a pre-trained biomedical language representation model for biomedical text mining. *Bioinformatics* 36, 4 (2020), 1234–1240.

[47] Dong Li, Guihong Wan, Xintao Wu, Xinyu Wu, Ajit J Nirmal, Christine G Lian, Peter K Sorger, Yevgeniy R Semenov, and Chen Zhao. 2025. A Survey on Computational Pathology Foundation Models: Datasets, Adaptation Strategies, and Evaluation Tasks. *arXiv preprint arXiv:2501.15724* (2025).

[48] Junnan Li, Dongxu Li, Silvio Savarese, and Steven Hoi. 2023. Blip-2: Bootstrapping language-image pre-training with frozen image encoders and large language models. In *International conference on machine learning*. PMLR, 19730–19742.

[49] Yuci Liang, Xinheng Lyu, Meidan Ding, Wenting Chen, Jipeng Zhang, Yuexiang Ren, Xiangjian He, Song Wu, Sen Yang, Xiyue Wang, et al. 2024. WSI-LLaVA: A Multimodal Large Language Model for Whole Slide Image. *arXiv preprint arXiv:2412.02141* (2024).

[50] Haotian Liu, Chunyuan Li, Yuheng Li, Bo Li, Yuanhan Zhang, Sheng Shen, and Yong Jae Lee. 2024. LLaVA-NeXT: Improved reasoning, OCR, and world knowledge. https://llava-vl.github.io/blog/2024-01-30-llava-next/

[51] Haotian Liu, Chunyuan Li, Qingyang Wu, and Yong Jae Lee. 2023. Visual instruction tuning. *Advances in neural information processing systems* 36 (2023), 34892–34916.

[52] Ze Liu, Yutong Lin, Yue Cao, Han Hu, Yixuan Wei, Zheng Zhang, Stephen Lin, and Baining Guo. 2021. Swin transformer: Hierarchical vision transformer using shifted windows. In *Proceedings of the IEEE/CVF international conference on computer vision*. 10012–10022.

[53] Ming Y Lu, Bowen Chen, Drew FK Williamson, Richard J Chen, Ivy Liang, Tong Ding, Guillaume Jaume, Igor Odintsov, Long Phi Le, Georg Gerber, et al. 2024. A visual-language foundation model for computational pathology. *Nature Medicine* (2024).

[54] Ming Y Lu, Bowen Chen, Drew FK Williamson, Richard J Chen, Melissa Zhao, Aaron K Chow, Kenji Ikemura, Ahrong Kim, Dimitra Pouli, Ankush Patel, et al. 2024. A multimodal generative AI copilot for human pathology. *Nature* 634, 8033 (2024), 466–473.

[55] Ming Y Lu, Bowen Chen, Andrew Zhang, Drew FK Williamson, Richard J Chen, Tong Ding, Long Phi Le, Yung-Sung Chuang, and Faisal Mahmood. 2023. Visual language pretrained multiple instance zero-shot transfer for histopathology images. In *Proceedings of the IEEE/CVF conference on computer vision and pattern recognition*. 19764–19775.

[56] Ruben T Lucassen, Sander PJ Moonemans, Tijn van de Luijtgaarden, Gerben E Breimer, Willeke AM Blokx, and Mitko Veta. 2025. Pathology Report Generation and Multimodal Representation Learning for Cutaneous Melanocytic Lesions. *arXiv preprint arXiv:2502.19293* (2025).

[57] Renqian Luo, Liai Sun, Yingce Xia, Tao Qin, Sheng Zhang, Hoifung Poon, and Tie-Yan Liu. 2022. BioGPT: generative pre-trained transformer for biomedical text generation and mining. *Briefings in bioinformatics* 23, 6 (2022), bbac409.

[58] Mieko Ochi, Daisuke Komura, and Shumpei Ishikawa. 2025. Pathology Foundation Models. *JMA journal* 8, 1 (2025), 121–130.

[59] Alec Radford, Jong Wook Kim, Chris Hallacy, Aditya Ramesh, Gabriel Goh, Sandhini Agarwal, Girish Sastry, Amanda Askell, Pamela Mishkin, Jack Clark, et al. 2021. Learning transferable visual models from natural language supervision. In *ICML*. PMLR.

[60] Lynn Marie Schriml, Cesar Arze, Suvarna Nadendla, Yu-Wei Wayne Chang, Mark Mazaitis, Victor Felix, Gang Feng, and Warren Alden Kibbe. 2012. Disease Ontology: a backbone for disease semantic integration. *Nucleic acids research* 40, D1 (2012), D940–D946.

[61] Christoph Schuhmann, Romain Beaumont, Richard Vencu, Cade Gordon, Ross Wightman, Mehdi Cherti, Theo Coombes, Aarush Katta, Clayton Mullis, Mitchell Wortsman, et al. 2022. Laion-5b: An open large-scale dataset for training next generation image-text models. *Advances in neural information processing systems* 35 (2022), 25278–25294.

[62] Mehmet Saygin Seyfioglu, Wisdom O Ikezogwo, Fatemeh Ghezloo, Ranjay Krishna, and Linda Shapiro. 2024. Quilt-llava: Visual instruction tuning by extracting localized narratives from open-source histopathology videos. In *Proceedings of the IEEE/CVF Conference on Computer Vision and Pattern Recognition*. 13183–13192.

[63] George Shaikovski, Adam Casson, Kristen Severson, Eric Zimmermann, Yi Kan Wang, Jeremy D Kunz, Juan A Retamero, et al. 2024. PRISM: A Multi-Modal Generative Foundation Model for Slide-Level Histopathology. *arXiv:2405.10254* (2024).

[64] Zhuchen Shao, Hao Bian, Yang Chen, Yifeng Wang, Jian Zhang, Xiangyang Ji, et al. 2021. Transmil: Transformer based correlated multiple instance learning for whole slide image classification. *Advances in neural information processing systems* 34 (2021), 2136–2147.

[65] Noam Shazeer, Azalia Mirhoseini, Krzysztof Maziarz, Andy Davis, Quoc Le, Geoffrey Hinton, and Jeff Dean. 2017. Outrageously large neural networks: The

[66] sparsely-gated mixture-of-experts layer. *arXiv preprint arXiv:1701.06538* (2017).

[66] Shenghuan Sun, Alexander Schubert, Gregory M Goldgof, Zhiqing Sun, Thomas Hartvigsen, Atul J Butte, and Ahmed Alaa. 2024. Dr-LLaVA: Visual Instruction Tuning with Symbolic Clinical Grounding. *arXiv preprint arXiv:2405.19567* (2024).

[67] Yuxuan Sun, Yixuan Si, Chenglu Zhu, Xuan Gong, Kai Zhang, Pingyi Chen, Ye Zhang, Zhongyi Shui, Tao Lin, and Lin Yang. 2024. CPath-Omni: A Unified Multimodal Foundation Model for Patch and Whole Slide Image Analysis in Computational Pathology. *arXiv preprint arXiv:2412.12077* (2024).

[68] Yuxuan Sun, Hao Wu, Chenglu Zhu, Sunyi Zheng, Qizi Chen, Kai Zhang, Yunlong Zhang, Dan Wan, Xiaoxiao Lan, Mengyue Zheng, et al. 2024. Pathmmu: A massive multimodal expert-level benchmark for understanding and reasoning in pathology. In *European Conference on Computer Vision*. Springer, 56–73.

[69] Yuxuan Sun, Yunlong Zhang, Yixuan Si, Chenglu Zhu, Zhongyi Shui, Kai Zhang, Jingxiong Li, Xinheng Lyu, Tao Lin, and Lin Yang. 2024. Pathgen-1.6 m: 1.6 million pathology image-text pairs generation through multi-agent collaboration. *arXiv preprint arXiv:2407.00203* (2024).

[70] Yuxuan Sun, Chenglu Zhu, Sunyi Zheng, Kai Zhang, Lin Sun, Zhongyi Shui, Yunlong Zhang, Honglin Li, and Lin Yang. 2024. Pathasst: A generative foundation ai assistant towards artificial general intelligence of pathology. In *AAAI*.

[71] Katarzyna Tomczak, Patrycja Czerwińska, and Maciej Wiznerowicz. 2015. Review The Cancer Genome Atlas (TCGA): an immeasurable source of knowledge. *Contemporary Oncology/Współczesna Onkologia* 2015, 1 (2015), 68–77.

[72] Hugo Touvron, Thibaut Lavril, Gautier Izacard, Xavier Martinet, Marie-Anne Lachaux, Timothée Lacroix, Baptiste Rozière, Naman Goyal, Eric Hambro, Faisal Azhar, et al. 2023. Llama: Open and efficient foundation language models. *arXiv preprint arXiv:2302.13971* (2023).

[73] Hugo Touvron, Louis Martin, Kevin Stone, Peter Albert, Amjad Almahairi, Yasmine Babaei, Nikolay Bashlykov, Soumya Batra, Prajjwal Bhargava, Shruti Bhosale, et al. 2023. Llama 2: Open foundation and fine-tuned chat models. *arXiv preprint arXiv:2307.09288* (2023).

[74] Manuel Tran, Paul Schmidle, Sophia J Wagner, Valentin Koch, Valerio Lupperger, Annette Feuchtinger, Alexander Böhner, Robert Kaczmarczyk, Tilo Biedermann, Kilian Eyerich, et al. 2024. Generating highly accurate pathology reports from gigapixel whole slide images with HistoGPT. *medRxiv* (2024), 2024–03.

[75] Anurag Vaidya, Andrew Zhang, Guillaume Jaume, Andrew H Song, Tong Ding, Sophia J Wagner, Ming Y Lu, Paul Doucet, Harry Robertson, Cristina Almagro-Perez, et al. 2025. Molecular-driven Foundation Model for Oncologic Pathology. *arXiv preprint arXiv:2501.16652* (2025).

[76] Eugene Vorontsov, Alican Bozkurt, Adam Casson, George Shaikovski, Michal Zelechowski, et al. 2023. Virchow: A million-slide digital pathology foundation model. *arXiv:2309.07778* (2023).

[77] Wenhui Wang, Hangbo Bao, Li Dong, Johan Bjorck, Zhiliang Peng, Qiang Liu, Kriti Aggarwal, Owais Khan Mohammed, et al. 2022. Image as a foreign language: Beit pretraining for all vision and vision-language tasks. *arXiv:2208.10442* (2022).

[78] Xiao Wang, Guangyao Chen, Guangwu Qian, Pengcheng Gao, Xiao-Yong Wei, Yaowei Wang, Yonghong Tian, and Wen Gao. 2023. Large-scale multi-modal pre-trained models: A comprehensive survey. *Machine Intelligence Research* 20, 4 (2023), 447–482.

[79] Xiyue Wang, Sen Yang, Jun Zhang, Minghui Wang, Jing Zhang, Wei Yang, Junzhou Huang, and Xiao Han. 2022. Transformer-based unsupervised contrastive learning for histopathological image classification. *Medical image analysis* (2022).

[80] Xiyue Wang, Junhan Zhao, Eliana Marostica, Wei Yuan, Jietian Jin, Jiayu Zhang, Ruijiang Li, Hongping Tang, Kanran Wang, Yu Li, et al. 2024. A pathology foundation model for cancer diagnosis and prognosis prediction. *Nature* (2024).

[81] Yang Wang. 2021. Survey on deep multi-modal data analytics: Collaboration, rivalry, and fusion. *ACM Transactions on Multimedia Computing, Communications, and Applications (TOMM)* 17, 1s (2021), 1–25.

[82] Jiayang Wu, Wensheng Gan, Zefeng Chen, Shicheng Wan, and S Yu Philip. 2023. Multimodal large language models: A survey. In *2023 IEEE International Conference on Big Data (BigData)*. IEEE, 2247–2256.

[83] Xiaomin Wu, Rui Xu, Pengchen Wei, Wenkang Qin, Peixiang Huang, Ziheng Li, and Lin Luo. 2024. Pathinsight: Instruction tuning of multimodal datasets and models for intelligence assisted diagnosis in histopathology. *arXiv preprint arXiv:2408.07037* (2024).

[84] Peng Xia, Kangyu Zhu, Haoran Li, Tianze Wang, Weijia Shi, Sheng Wang, Linjun Zhang, James Zou, and Huaxiu Yao. 2024. Mmed-rag: Versatile multimodal rag system for medical vision language models. *arXiv preprint arXiv:2410.13085* (2024).

[85] Jinxi Xiang, Xiyue Wang, Xiaoming Zhang, Yinghua Xi, Feyisope Eweje, Yijiang Chen, Yuchen Li, Colin Bergstrom, Matthew Gopaulchan, Ted Kim, et al. 2025. A vision–language foundation model for precision oncology. *Nature* (2025).

[86] Yingxue Xu, Yihui Wang, Fengtao Zhou, Jiabo Ma, Shu Yang, Huangjing Lin, Xin Wang, Jiguang Wang, Li Liang, Anjia Han, et al. 2024. A multimodal knowledge-enhanced whole-slide pathology foundation model. *arXiv preprint arXiv:2407.15362* (2024).

[87] An Yang, Baosong Yang, Beichen Zhang, Binyuan Hui, Bo Zheng, Bowen Yu, Chengyuan Li, Dayiheng Liu, Fei Huang, Haoran Wei, et al. 2024. Qwen2. 5 technical report. *arXiv preprint arXiv:2412.15115* (2024).

[88] Fan Yang, Wenchuan Wang, Fang Wang, Yuan Fang, Duyu Tang, Junzhou Huang, Hui Lu, and Jianhua Yao. 2022. scBERT as a large-scale pretrained deep language model for cell type annotation of single-cell RNA-seq data. *Nature Machine Intelligence* 4, 10 (2022), 852–866.

[89] Jiahui Yu, Zirui Wang, Vijay Vasudevan, Legg Yeung, Mojtaba Seyedhosseini, and Yonghui Wu. 2022. Coca: Contrastive captioners are image-text foundation models. *arXiv preprint arXiv:2205.01917* (2022).

[90] Xiaohua Zhai, Basil Mustafa, Alexander Kolesnikov, and Lucas Beyer. 2023. Sigmoid loss for language image pre-training. In *Proceedings of the IEEE/CVF international conference on computer vision.* 11975–11986.

[91] Kai Zhang, Rong Zhou, Eashan Adhikarla, Zhiling Yan, Yixin Liu, Jun Yu, Zhengliang Liu, Xun Chen, Brian D Davison, Hui Ren, et al. 2024. A generalist vision–language foundation model for diverse biomedical tasks. *Nature Medicine* (2024), 1–13.

[92] Pan Zhang, Xiaoyi Dong, Bin Wang, Yuhang Cao, Chao Xu, Linke Ouyang, Zhiyuan Zhao, Haodong Duan, Songyang Zhang, Shuangrui Ding, et al. 2023. Internlm-xcomposer: A vision-language large model for advanced text-image comprehension and composition. *arXiv preprint arXiv:2309.15112* (2023).

[93] Sheng Zhang, Yanbo Xu, Naoto Usuyama, Hanwen Xu, Jaspreet Bagga, Robert Tinn, Sam Preston, Rajesh Rao, Mu Wei, Naveen Valluri, et al. 2023. Biomedclip: a multimodal biomedical foundation model pretrained from fifteen million scientific image-text pairs. *arXiv preprint arXiv:2303.00915* (2023).

[94] Theodore Zhao, Yu Gu, Jianwei Yang, Naoto Usuyama, Ho Hin Lee, Sid Kiblawi, Tristan Naumann, Jianfeng Gao, Angela Crabtree, Jacob Abel, et al. 2024. A foundation model for joint segmentation, detection and recognition of biomedical objects across nine modalities. *Nature methods* (2024), 1–11.

[95] Lianmin Zheng, Wei-Lin Chiang, Ying Sheng, Siyuan Zhuang, Zhanghao Wu, Yonghao Zhuang, Zi Lin, Zhuohan Li, Dacheng Li, Eric Xing, et al. 2023. Judging llm-as-a-judge with mt-bench and chatbot arena. *Advances in Neural Information Processing Systems* 36 (2023), 46595–46623.

[96] Jinghao Zhou, Chen Wei, Huiyu Wang, Wei Shen, Cihang Xie, Alan Yuille, and Tao Kong. 2021. ibot: Image bert pre-training with online tokenizer. *arXiv:2111.07832* (2021).

[97] Qifeng Zhou, Thao M Dang, Wenliang Zhong, Yuzhi Guo, Hehuan Ma, Saiyang Na, and Junzhou Huang. 2025. MLLM4PUE: Toward Universal Embeddings in Computational Pathology through Multimodal LLMs. *arXiv preprint arXiv:2502.07221* (2025).

[98] Xiao Zhou, Luoyi Sun, Dexuan He, Wenbin Guan, Ruifen Wang, and Lifeng others Wang. 2024. A Knowledge-enhanced Pathology Vision-language Foundation Model for Cancer Diagnosis. *arXiv preprint arXiv:2412.13126* (2024).

[99] Xiao Zhou, Xiaoman Zhang, Chaoyi Wu, Ya Zhang, Weidi Xie, and Yanfeng Wang. 2024. Knowledge-enhanced visual-language pretraining for computational pathology. In *ECCV.* Springer.

[100] Eric Zimmermann, Eugene Vorontsov, Julian Viret, Adam Casson, Michal Zelechowski, et al. 2024. Virchow2: Scaling self-supervised mixed magnification models in pathology. *arXiv:2408.00738* (2024).